

Stimulating photosynthetic processes increases productivity and water use efficiency in the field

Patricia E. López-Calcano^{1,2*}, Kenny L. Brown^{1,2}, Andrew J. Simkin^{1,2,3}, Stuart J. Fisk², Silvere Vialet-Chabrand², Tracy Lawson², Christine A. Raines^{2*}

¹ P.E.L.C, K.L.B. and A.J.S contributed equally to this work

² School of Life Sciences, Wivenhoe Park, University of Essex, Colchester, CO4 3SQ, UK.

³ Genetics, Genomics and Breeding, NIAB EMR New Road, East Malling, Kent, ME19 6BJ.

* Address correspondence to C.A.R. (email: rainc@essex.ac.uk) or to P.E.L.C. (email: pelope@essex.ac.uk).

Short title: Improving photosynthesis and yield

ORCID IDs: 0000-0003-2436-8988 (P.E.L.C); 0000-0002-0587-2698 (K.L.B.); 0000-0001-5056-1306 (A.J.S.); 0000-0002-2105-2825 (S.V.C); 0000-0002-4073-7221 (T.L.); 0000-0001-7997-7823 (C.A.R)

One sentence summary: Simultaneous stimulation of RuBP regeneration and electron transport results in improvements in biomass yield in glasshouse and field grown tobacco.

23 **Abstract**

24 Previous studies have demonstrated that independent stimulation of either electron transport
25 or RuBP regeneration can increase the rate of photosynthetic carbon assimilation and plant
26 biomass. In this paper, we present evidence that a multi-gene approach to simultaneously
27 manipulate these two processes provides a further stimulation of photosynthesis. We report
28 on the introduction of the cyanobacterial bifunctional enzyme fructose-1, 6-
29 biphosphatase/sedoheptulose-1,7-bisphosphatase or overexpression of the plant enzyme
30 sedoheptulose-1,7-bisphosphatase, together with expression of the red algal protein
31 cytochrome c_6 , and show that a further increase in biomass accumulation under both
32 glasshouse and field conditions can be achieved. Furthermore, we provide evidence that
33 stimulation of both electron transport and RuBP regeneration can lead to enhanced intrinsic
34 water use efficiency under field conditions.

35

36 **Keywords:** SBPase; FBP/SBPase; Calvin-Benson cycle; cytochrome c_6 ; chlorophyll
37 fluorescence imaging; transgenic; electron transport; biomass; water use efficiency.

Yield potential of seed crops grown under optimal management practices, and in the absence of biotic and abiotic stress, is determined by incident solar radiation over the growing season, the efficiency of light interception, energy conversion efficiency and partitioning or harvest index. For the major crops, the only component not close to the theoretical maximum is energy conversion efficiency, which is determined by gross canopy photosynthesis minus respiration. This highlights photosynthesis as a target for improvement to raise yield potential in major seed crops¹⁻³.

Transgenic experiments and modelling studies have provided compelling evidence that increasing the levels of photosynthetic enzymes in the Calvin Benson (CB) cycle has the potential to impact photosynthetic rate and yield^{1,2,4-15}. Over-expression of SBPase in tobacco^{5,7,8}, Arabidopsis⁹, tomato¹⁵ and wheat¹⁶ has demonstrated the potential of manipulating the expression of CB cycle enzymes and specifically the regeneration of RuBP to increase growth, biomass (30-42%) and even seed yield (10-53%). Similarly, overexpression of other enzymes including FBPA¹⁴, cyanobacterial SBPase, FBPase¹⁷ and the bifunctional fructose-1,6-bisphosphatases/sedoheptulose-1,7-bisphosphatase (FBP/SBPase^{4,18,19}) in a range of species has shown that increasing photosynthesis increases yield. In addition to manipulation of CB cycle genes, increasing photosynthetic electron transport has also been shown to have a beneficial effect on plant growth. Overexpression of the Rieske FeS protein -a key component of the cytochrome *b₆f* complex- in Arabidopsis, has previously been shown to lead to increases in electron transport rates, CO₂ assimilation, biomass and seed yield²⁰. Similar results were also observed when the Rieske FeS protein was over-expressed in the C4 plant *Setaria viridis* demonstrating that this manipulation has the potential to have a positive effect in both C3 and C4 species²¹. Furthermore, the introduction of the algal cytochrome *c₆* protein into Arabidopsis and tobacco resulted in

increased growth^{22,23}. In cytochrome c_6 expressing transgenic plants, the electron transport rate was increased along with ATP, NADPH, chlorophyll, starch content, and capacity for CO₂ assimilation. Higher plants have been proposed to have lost the cytochrome c_6 protein through evolution, but in green algae and cyanobacteria, which have genes for both cytochrome c_6 and plastocyanin (PC), cytochrome c_6 has been shown to replace PC as the electron transporter connecting the cytochrome b_6/f complex with PSI under Cu deficiency conditions^{24,25}. There is evidence showing that PC can limit electron transfer between cytochrome b_6/f complex and PSI²⁶, and in Arabidopsis, it has been shown that introduced algal cytochrome c_6 is a more efficient electron donor to P700 than PC²². This evidence suggests the introduction of the cytochrome c_6 protein in higher plants as a viable strategy for improving photosynthesis.

This paper aims to test the hypothesis that combining an increase in the activity of a CB cycle enzyme, specifically enhancing RuBP regeneration, together with stimulation of the electron transport chain can boost photosynthesis and yield above that observed when these processes are targeted individually. *Nicotiana tabacum* plants expressing the cyanobacterial FBP/SBPase or the higher plant SBPase, and the algal cytochrome c_6 were generated using two different tobacco cultivars. The analysis presented here demonstrates that the simultaneous stimulation of electron transport and RuBP regeneration leads to a significant increase in photosynthetic carbon assimilation, and results in increased biomass and yield under both glasshouse and field conditions.

Production and Selection of Tobacco Transformants

Previous differences observed in the biomass accumulation between *Arabidopsis* and tobacco overexpressing SBPase and SBPase plus FBPA^{8,9} led us to explore the effect of similar manipulations (RuBP regeneration by overexpression of SBPase or introduction of the cyanobacterial FBP/SBPase, together with enhanced electron transport) in two different tobacco cultivars with different growth habits: *N. tabacum* cv. Petite Havana, with indeterminate growth, and *N. tabacum* cv. Samsun, with determinate growth. Sixty lines of cv. Petit Havana, and up to fourteen lines of cv. Samsun were generated per construct and T0 and T1 transgenic tobacco were screened by qPCR and immuno-blot analysis to select independent lines with expression of the transgenes (data not shown).

N. tabacum cv. Petit Havana T2/T3 progeny expressing FBP/SBPase (S_B ; lines S_{B03} , S_{B06} , S_{B21} , S_{B44}) or cytochrome c_6 (C_6 ; lines C_{15} , C_{41} , C_{47} , C_{50}) and cv. Samsun lines expressing SBPase + cytochrome c_6 (SC_6 , lines SC_1 , SC_2 and SC_3) were produced by agrobacterium transformation. *N. tabacum* cv. Petit Havana plants expressing both S_B and C_6 were generated by crossing S_B lines (S_{B06} , S_{B21} , S_{B44}) with C_6 lines (C_{15} , C_{47} , C_{50}) to generate four independent $S_B C_6$ lines: S_{BC1} ($S_{B06} \times C_{47}$), S_{BC2} ($S_{B06} \times C_{50}$), S_{BC3} ($S_{B44} \times C_{47}$) and S_{BC6} ($S_{B21} \times C_{15}$). Semi-quantitative RT-PCR was used to detect the presence of the FBP/SBPase transcript in lines S_B and $S_B C_6$, cytochrome c_6 in lines C_6 , $S_B C_6$ and SC_6 , and SBPase in lines S and SC_6 (**Supplementary Fig. 1**). The selected S_B and $S_B C_6$ lines were shown to accumulate FBP/SBPase protein, and S and SC_6 to overexpress the SBPase protein by immunoblot analysis (**Fig. 1a and Supplementary Fig. 2**). In addition to immunoblot analysis, we analysed total extractable FBPase activity in the leaves of the cv. Petite Havana T2/T3 & F3 homozygous progeny lines used to determine chlorophyll fluorescence and photosynthetic parameters. This analysis showed that these plants (S_B and $S_B C_6$) had increased levels of FBPase activity ranging from 34 to 47% more than the control plants (**Fig.**

109 **1c).** The full set of assays showing the variation in FBPase activities between plants can be
110 seen in supplemental data (**Supplementary Fig. 3**). The S and SC₆ lines were from the same
111 generation of transgenic plants used in a previous study and shown to have increased SBPase
112 activity⁸. The cytochrome *c*₆ antibody (raised against a peptide from the *Porphyra umbilicalis*
113 protein) was unable to detect less than 60 ng of purified cytochrome *c*₆ protein extracted from
114 *E. coli* (**Supplementary Fig. 4**), and immunoblotting of leaf extracts did not result in a
115 signal. However, when semi-purified extracts from lines C15, C41 and C47 were used, a
116 band of the expected molecular weight was identified in semi-purified extracts from lines
117 C15, C41 and C47, providing qualitative confirmation of the presence of cytc6 in the
118 transgenic tobacco plants (**Fig. 1b and Supplementary Fig. 5a**). No bands were observed in
119 semi-purified extracts from control (CN) plants. To provide further evidence of the presence
120 of introduced cytochrome *c*₆ protein a spectral scan was run using the semi-purified protein
121 extracts of C₆ and CN plants; the sorot peak at 420 nm demonstrated the presence of the heme
122 group and was only detectable in the C₆ transgenic plants and not in the CN plants.
123 (**Supplementary Fig. 5b**). Additionally, a physiological assay probing the response of
124 photosynthesis during light induction was performed. CN and C₆ plants were provided with
125 saturating light and [CO₂] following a period of darkness. The C₆ plants were shown to have
126 both a more rapid response and greater rate of net CO₂ assimilation compared with CN plants
127 (**Supplementary Fig. 6a & 6d**). The faster increase in *A* was accompanied by a quicker rise
128 in the operating efficiency of both PSII (F_q'/F_m') and PSI (YI) providing evidence that in
129 these plants electron flow through both photosystems was increased. This increase in electron
130 transport could contribute to the higher *A* rates observed by providing the required energy
131 (ATP) and reductant (NADPH). This response was further accelerated in S_BC₆ transgenic
132 plants mostly likely due to the increased sink capacity provided by CB cycle activity
133 (**Supplementary Fig. 6**).

Chlorophyll fluorescence analysis confirmed that in young plants, the operating efficiency of photosystem two (PSII) photochemistry F_q'/F_m' at an irradiance of 600-650 $\mu\text{mol m}^{-2} \text{s}^{-1}$ was significantly higher in all selected lines compared to either WT or null segregant controls (**Fig. 1d, e**). However, the F_q'/F_m' values of the $S_B C_6$ and SC_6 lines, were not significantly different from the F_q'/F_m' values obtained from the plants expressing individually FBP/SBPase (S_B), cytochrome c_6 (C_6) or SBPase (S).

Stimulation of electron transport and RuBP regeneration increases photosynthesis

Transgenic lines selected based on the initial screens described above were grown in the glasshouse, in natural light supplemented to provide illumination between 400-1000 $\mu\text{mol m}^{-2} \text{s}^{-1}$. The rate of net CO_2 assimilation (A) and F_q'/F_m' was determined as a function of internal CO_2 concentration (C_i), in mature and developing leaves of *N. tabacum* cv. Samsun (S and SC_6) and in mature leaves of *N. tabacum* cv. Petit Havana (S_B , C_6 and $S_B C_6$) (**Fig. 2**). The transgenic plants displayed greater CO_2 assimilation rates than those of the control (CN) plants. A was 15% higher than the controls in the mature leaves of the SC_6 , at a C_i of approximately 300 $\mu\text{mol mol}^{-1}$ (the C_i prevailing at current atmospheric $[\text{CO}_2]$) (**Fig. 2b**). The developing leaves of the SC_6 plants also showed significant increases in PSII operating efficiency (F_q'/F_m') and in the PSII efficiency factor (F_q'/F_v' ; which is determined by the ability of the photosynthetic apparatus to maintain Q_A in the oxidized state and therefore a measure of photochemical quenching) when compared to control plants (**Fig. 2c**). Interestingly, in mature leaves of the cv. Samsun transgenic plants, the differences in assimilation rates and in the operating efficiency of PSII photochemistry between the transgenic and the CN plants were smaller than in the developing leaves. Only the S transgenic plants displayed a higher average value for F_q'/F_m' and F_q'/F_v' than the CN plants

at all CO₂ concentrations measured. In contrast, the mature leaves of SC₆ plants displayed F_q'/F_v' values higher than the control only at C_i levels between 300 and 900 µmol mol⁻¹ (**Fig. 2b**).

Similar trends were shown for the *N. tabacum* cv. Petit Havana transgenic plants, which displayed higher average values of A and F_q'/F_m' than the CN (**Fig. 2a**). In the leaves of the S_BC₆ plants (cv. Petit Havana) these significant increases were similar to the developing leaves of the SC₆ lines (cv. Samsun). No significant differences in PSII maximum efficiency (F_v'/F_m') were observed between the CN and the transgenics in either cultivar.

The developing leaves of both the S and SC₆ plants (cv. Samsun) showed a significant increase in both the maximum electron transport and RuBP regeneration rate (J_{max}) and maximum assimilation (A_{max}) when compared the control plants (**Table 1**). The mature leaves of the SC₆ (cv. Samsun) and S_BC₆ (cv. Petite Havana) transgenics also displayed a significantly higher A_{max} than the CN, and higher average values for $V_{C_{max}}$, and J_{max} were also evident in these leaves. These results showed that simultaneous stimulation of electron transport and RuBP regeneration by expression of cytochrome *c₆* in combination with FBP/SBPase or SBPase has a greater impact on photosynthesis than the single manipulations in all plants analysed.

Stimulation of electron transport and RuBP regeneration improves growth

In parallel experiments, plants expressing FBP/SBPase (S_B), cytochrome *c₆* (C₆) and both (S_BC₆) (*N. tabacum* cv. Petite Havana) and plants expressing SBPase (S) and SBPase + cytochrome *c₆* (SC₆) (*N. tabacum* cv. Samsun) were grown in the glasshouse for four and six weeks respectively before harvesting. Height, leaf number, total leaf area and above ground biomass were determined (**Fig 3** and **Supplementary Fig 7**). All of the transgenic plants analysed here displayed increased height when compared to CN plants. Plants expressing

cytochrome c_6 (C_6 , $S_B C_6$, (cv. Petite Havana) and SC_6 (cv. Samsun)) had a significant increase in leaf area and in stem and leaf biomass compared to their respective controls (**Fig.3** and **Supplementary Fig. 8,9**). In the S_B transgenic plants (cv. Petite Havana) only the biomass of the stem was greater than the CN plants. Notably the $S_B C_6$ and SC_6 transgenics displayed significantly greater leaf area than the single S_B and S transgenic plants respectively. The total increase in above ground biomass when compared to CN group was 35% in S_B , 44% in C_6 and 9% in S , with consistently higher means in the double manipulations $S_B C_6$ (52%) and SC_6 (32%) (**Fig.3**).

Expression of FBP/SBPase and cytochrome c_6 increases growth and water use efficiency

To test whether the increases in biomass observed in these transgenic plants under glasshouse conditions could be reproduced in a field environment, a subset of lines was selected for testing in the field. Since the larger percentage increases in biomass were displayed by the manipulations in *N. tabacum* cv. Petit Havana, these plants were selected and tested in three field experiments in two different years (2016 and 2017).

In 2016, a small-scale replicated control experiment was carried out to evaluate vegetative growth in the field, in the lines expressing single gene constructs for FBP/SBPase (S_B) and cytochrome c_6 (C_6) (**Supplementary Fig. 14a**). Plants were germinated and grown under controlled environment conditions for 25 d before being moved to the field. After 14 d in the field, plants were harvested at an early vegetative stage and plant height, total leaf area and above ground biomass were measured (**Fig. 4 (a-c)** and **Supplementary Fig. 10a**). These data revealed that the S_B and C_6 plants showed an increase in height, leaf area and above ground biomass of 27%, 35% and 25% respectively for S_B and 50%, 41% and 36% respectively for C_6 when compared to CN plants.

In 2017, two larger scale, randomized block design field experiments were carried out to evaluate performance in the S_B , C_6 and S_BC_6 plants compared to CN plants (**Supplementary Fig.14b**). Plants were grown from seed in the glasshouse for 33 d, and then moved to the field and allowed to grow until the onset of flowering (further 24-33 d), before harvesting. In **Fig. 4d-i** it can be seen that the S_B and C_6 plants harvested after the onset of flowering did not display any significant increases in height, leaf area or biomass when compared to CN plants. Interestingly, plants expressing both FBP/SBPase and cytochrome c_6 (S_BC_6), displayed a significant increase in a number of growth parameters; with 13%, 17% and 27% increases in height, leaf area and above ground biomass respectively when compared to CN plants.

Additionally, in the 2017 field experiments A as a function of C_i at saturating light (A/C_i) was determined. In the 2017 Experiment 1 a significant increase in A was observed in S_B and C_6 plants without differences in PSII operating efficiency (F_q'/F_m') (**Fig. 5a**). However, in the 2017 Experiment 2, no differences in A or in F_q'/F_m' values were evident in the C_6 and S_BC_6 plants when compared to the CN plants (**Fig. 5b**). Analysis of A as a function of light (A/Q) showed either small or no significant differences in A between genotypes (**Fig. 6a** and **Supplementary Fig 11a**). Interestingly, g_s in the S_BC_6 plants was significantly lower than for the C_6 and CN plants at light intensities above $1000 \mu\text{mol m}^{-2} \text{s}^{-1}$ (**Fig 6b**), resulting in a significant increase in intrinsic water use efficiency ($iWUE$) for S_BC_6 plants (**Fig 6d**). No significant differences in $iWUE$ were observed for S_B or C_6 transgenic plants (**Fig 6d** and **Supplementary Fig 11d**).

DISCUSSION

In this study, we describe the generation and analysis of transgenic plants with simultaneous increases in electron transport and improved capacity for RuBP regeneration, in two different tobacco cultivars. Here we have shown that independent stimulation of electron transport (by expression of cytochrome c_6) and stimulation of RuBP regeneration (by expression of FBP/SBPase or overexpression of SBPase) increased photosynthesis and biomass in glasshouse studies. Furthermore, we demonstrated how the targeting of these two processes simultaneously (in the $S_B C_6$ and SC_6 plants) had an even greater effect in stimulating photosynthesis and growth. Additionally, in field studies we demonstrate that plants with simultaneous stimulation of electron transport and of RuBP regeneration had increased *iWUE* with an increase in biomass.

Under glasshouse conditions, increases in photosynthesis were observed in all of the transgenic plants analysed here and this was found to be correlated with increased biomass. Although increases in photosynthesis and biomass have been reported for plants with stimulation of RuBP regeneration in both model^{4,5,8,7,27} and crop^{18,16} species; and electron transport in Arabidopsis and tobacco^{20,22,28}, the data presented here provides the first report of increased photosynthesis and biomass by the simultaneous stimulation of electron transport and RuBP regeneration. Increases in *A* were observed under glasshouse conditions in the leaves of all of the different transgenic tobacco plants and in both tobacco cultivars (cv. Petit Havana and cv. Samsun). Analysis of the *A/C_i* response curves showed that the average values for the photosynthetic parameters $V_{C_{max}}$, J_{max} and A_{max} increased by up to 11, 14 and 15% respectively. These results indicated that not only was the maximal rate of electron transport and RuBP regeneration increased, but the rate of carboxylation by Rubisco was also increased. Although this may seem counterintuitive in that we have not targeted directly

Rubisco activity, it is in keeping with a study by Wullschleger²⁹ of over 100 plant species that showed a linear correlation between J_{\max} and $V_{C_{\max}}$. Furthermore, it has also been shown previously that overexpression of SBPase leads not only to a significant increase in J_{\max} but that an increase in $V_{C_{\max}}$ and Rubisco activation state^{5,8}.

Notably, in the greenhouse study, the highest photosynthetic rates were observed in plants in which both electron transport and RuBP regeneration ($S_B C_6$ and SC_6) were boosted, suggesting that the co-expression of these genes results in an additive effect on improving photosynthesis. In addition to the increases in A , the plants with simultaneous stimulation of electron transport and RuBP regeneration displayed a significant increase in F_q'/F_m' , indicating a higher quantum yield of linear electron flux through PSII compared to the control plants. These results are in keeping with the published data for the introduction of cytochrome c_6 and the overexpression of the Rieske FeS protein in Arabidopsis^{20,22}. In these studies the plants had a higher quantum yield of PSII and a more oxidised plastoquinone pool²², suggesting that, although PC is not always limiting under all growth conditions³⁰, there is scope to stimulate reduction of PSI by using alternative, more efficient electron donors to PSI like cytochrome c_6 ^{22,26}. Furthermore, in the $S_B C_6$ and SC_6 plants the increase in F_q'/F_m' was found to be largely driven by the increase in the PSII efficiency factor (F_q'/F_v'). This suggests that the increase in efficiency in these plants is likely due to stimulation of processes down stream of PSII such as CO_2 assimilation.

To provide further evidence of the applicability of targeting both electron transport and RuBP regeneration to improve crop yields, we tested these plants in the field. Here we showed that the expression FBP/SBPase alone led to an increase in growth and biomass in the 2016 field-grown plants of between 22-40%, when harvested during early vegetative

growth, prior to the onset of flowering. Interestingly, when these plants were harvested later in development, after the onset of flowering, in the 2017 field trials, this advantage was no longer evident and the single FBP/SBPase expressors were indistinguishable from the control plants. These results are in contrast to the 2016 field data and may be due to the later timing in development of the harvest in the 2017 experiment. The transgenic plants expressing cytochrome *c*₆ alone also showed enhanced growth and biomass early development, but as with the FBPase/SBPase plants, this improvement was no longer evident when plants were harvested after flowering. This difference in biomass gain between the early and late harvest was not observed in a parallel experiment, where the overexpression of H-protein was shown to increase biomass under field conditions in plants harvested in early development and after the onset of flowering³¹. These results suggest that the expression of FBP/SBPase or cytochrome *c*₆ alone, may provide an advantage under particular sets of conditions or at specific stages of plant development. This might be exploitable for some crops where an early harvest is desirable (eg. some types of lettuce, spinach and tender greens)¹⁸. In contrast to the results with the single manipulations described above, plants expressing both cytochrome *c*₆ and FBP/SBPase simultaneously displayed a consistent increase in biomass after flowering under field conditions.

In the transgenic lines grown in the field, the correlation between increases in photosynthesis and increased biomass were less consistent than that observed under glasshouse conditions. The significant increases in photosynthetic capacity displayed by the FBP/SBPase and cytochrome *c*₆ expressors in 2017 Experiment 1, provided clear evidence that these individual manipulations are able to significantly stimulate photosynthetic performance under field conditions. However, no increase in biomass was evident in these plants. In contrast, in the 2017 Experiment 2 we did not detect any significant differences in

304 photosynthetic capacity in either the cytochrome c_6 expressors or the plants with
305 simultaneous expression of FBP/SBPase + cytochrome c_6 expressors, but increased biomass
306 was evident. At this point we have no explanation for this disparity. However, although not
307 significantly different, in all experiments, the mean A values of the transgenic plants were
308 consistently higher than those of the controls. It is known that even small increases in
309 assimilation throughout the lifetime of a plant will have a cumulative effect, which could
310 translate into a significant biomass accumulation⁸, this may in part explain the disparity with
311 the biomass results presented. Furthermore, the phenotyping experiments carried out on C_6
312 and $S_B C_6$ plants (**Supplementary Fig 6**) showed that there was a more rapid induction of
313 photosynthesis, particularly in $S_B C_6$ plants. This characteristic might also contribute to an
314 increase in photosynthetic rates and biomass when plants are grown in fluctuating light
315 conditions, but would not be detectable in the steady-state measurements performed in our
316 field experiments.

317
318
319 An unexpected result that was found in the plants with simultaneous expression of
320 FBP/SBPase + cytochrome c_6 ($S_B C_6$), is that these plants had a lower g_s and lower C_i at light
321 intensities above $1000 \mu\text{mol m}^{-2} \text{s}^{-1}$, when compared to control plants. Normally, lower C_i
322 would be expected to lead to a reduction in photosynthesis, but the $S_B C_6$ plants were able to
323 maintain CO_2 assimilation rates equal to or higher than control plants resulting in an
324 improvement in $iWUE$. A similar improvement in $iWUE$ was seen in plants overexpressing
325 the NPQ related protein, PsbS³². It was shown that light-induced stomatal opening was
326 reduced in these plants in which a more oxidized Q_A pool was found and this has been
327 proposed to act as a signal in stomatal movement³³. This higher $iWUE$ and the fact that a
328 higher productivity than controls has been reported in field studies for transgenic lines with

329 increased RuBP regeneration grown under CO₂ enrichment^{7,18}, highlight the potential of
330 manipulating electron transport and RuBP regeneration in the development of new varieties
331 able to sustain photosynthesis and yields under climate change scenarios.

MATERIALS AND METHODS

Generation of constructs and transgenic plants

Constructs were generated using Golden Gate cloning^{34,35} or Gateway cloning technology³⁶. Transgenes were under the control of CaMV35S and FMV constitutive promoters. Construct detail below and in **Supplementary Fig. 12**.

For *N. tabacum* cv. Petit Havana, the codon optimised cyanobacterial bifunctional fructose-1,6-bisphosphatases/sedoheptulose-1,7-bisphosphatase (FBP/SBPase; *slr2094* Synechocystis sp. PCC 7942⁴ linked to the geraniol synthase transit peptide³⁷ and the codon optimised *P. umbilicalis*'s cytochrome *c*₆ (AFC39870) with the chlorophyll a-b binding protein 6 transit peptide from Arabidopsis (AT3G54890) were used to generate Golden Gate³⁵ over-expression constructs (EC23083 and EC23028) driven by the FMV³⁸ and CaMV 35S promoters respectively (**Supplementary Fig. 12a**).

The cytochrome *c*₆ from *P. umbilicalis* was selected as it is commonly found on the UK coastline and it shares over 86% identity with previously published *P. yeoensis* and *Ulva fasciata* used by Chida *et al*²² and Yadav *et al*²³. The level of similarity between these proteins and the fact that the functional regions are identical, provides confidence that the cytochrome *c*₆ proteins from these three species function in a similar way (see alignment in **Supplementary Fig. 13**). The *P. umbilicalis* cytochrome *c*₆ was linked to the transit peptide from the light-harvesting complex I chlorophyll a/b binding protein 6 (At3g54890) to generate an over-expression construct driven by the CaMV 35S promoter; B2-C6 in the vector pGWB2³⁶ used for *N. tabacum* cv. Samsun transformation (**Supplementary Fig. 12b**). The recombinant plasmid B2-C6, was introduced into SBPase over-expressing tobacco cv. Samsun⁵ using *Agrobacterium tumefaciens* AGL1 via leaf-disc transformation³⁹. Primary transformants (39) (T0 generation) were regenerated on MS medium containing kanamycin

(100 mg L⁻¹), hygromycin (30 mg L⁻¹) and augmentin (500 mg L⁻¹). Plants expressing the integrated transgenes were screened using RT-PCR (data not shown).

Similarly, the recombinant plasmids EC23083, and EC23028 were introduced into wild type tobacco (*Nicotiana tabacum*) cv Petit Havana, using *A. tumefaciens* strain LBA4404 via leaf-disc transformation³⁹, and shoots regenerated on MS medium containing, hygromycin (20 mg L⁻¹) and cefotaxime (400 mg L⁻¹). Hygromycin resistant primary transformants (T0 generation) with established root systems were transferred to soil and allowed to self-fertilize.

Between twelve and 60 independent lines were generated per construct and 3-4 lines taken forward for further analysis. Control (CN) plants used in this study were a combination of WT and null segregant plants from the transgenic lines, verified by PCR for non-integration of the transgene.

Plant Growth

Controlled conditions

Wild-type tobacco plants and T1 progeny resulting from self-fertilization of transgenic plants were grown to seed in soil (Levington F2, Fisons, Ipswich, UK). Lines of interest were identified by immunoblot and qPCR. For the experiments in the Samsun cv. the null segregants were selected from transformed lines. For Petit Havana, the null segregants were selected from the S_BC₆ lines. For experimental study, T2-T4 and F1-F3 progeny seeds were germinated on soil in controlled environment chambers at an irradiance of 130 μmol photons m⁻² s⁻¹, 22°C, relative humidity of 60%, in a 16-h photoperiod. Plants were transferred to individual 8 cm pots and grown for two weeks at 130 μmol photons m⁻² s⁻¹, 22°C, relative humidity of 60%, in a 16-h photoperiod. Plants were transferred to 4 L pots and cultivated in a controlled environment glasshouse (16-h photoperiod, 25°C-30°C

day/20°C night, and natural light supplemented under low light induced by cloud cover with high-pressure sodium light bulbs, giving 380-1000 $\mu\text{mol m}^{-2} \text{s}^{-1}$ (high-light) from the pot level to the top of the plant, respectively). Positions of the plants were changed 3 times a week and watered regularly with a nutrient medium⁴⁰. Plants were positioned such that at maturity, a near-to-closed canopy was achieved and the temperature range was maintained similar to the ambient external environment. Four leaf discs (0.8 cm diameter) were taken for immunoblot analysis and FBPase activity. These disks were taken from the same areas of the leaf used for photosynthetic measurements, immediately plunged into liquid N₂ and stored at -80°C.

Field studies

Plants were grown as described in Lopez-Calcano et al³¹, and with a methodology broadly analogous to that used commercially for this crop. The field site was situated at the University of Illinois Energy Farm (40.11°N, 88.21°W, Urbana, IL). Two different experimental designs were used in 2 different years.

2016: Replicated control design (**Supplementary Fig. 14a**). Plants were grown in rows, spaced 30 cm apart with the outer boundary being a wild-type border. The entire experiment was surrounded by two rows of wild-type borders. Plants were irrigated when required using rain towers. T2 seed was germinated and after 11 d were moved to individual pots (350 mL). The seedlings were grown in the glasshouse for further 15 d before being moved into the field, and allowed to grow in the field for 14 d before harvest.

2017: Two experiments were carried out two weeks apart. A blocks-within-rows design was used (**Supplementary Fig. 14b**) where 1 block holds one line of each of the five manipulations and each row has all lines. The central 20 plants of each block are divided into five rows of four plants per genotype. The 2017 Exp.1 contained controls (WT and null

segregants), FBP/SBPase expressing lines (S_B) and cytochrome c_6 expressing lines (C_6). The 2017 Exp. 2 contained controls (WT and null segregants), cytochrome c_6 expressing lines (C_6), and FBP/SBPase + cytochrome c_6 expressing lines ($S_B C_6$). Seed was germinated and after 12 d moved to hydroponic trays (Trans-plant Tray GP009 6912 cells; Speedling Inc., Ruskin, FL), and grown in the glasshouse for 20 d before being moved to the field. The plants were allowed to grow in the field until flowering (approximately 30 d) before harvest.

The field was prepared in a similar fashion each year as described in Kromdijk *et al*⁴¹. Light intensity (LI-quantum sensor; LI-COR) and air temperature (Model 109 temperature probe; Campbell Scientific Inc, Logan, UT) were measured nearby on the same field site, and half-hourly averages were logged using a data logger (CR1000; Campbell Scientific).

cDNA generation and RT-PCR

Total RNA was extracted from tobacco leaf disks (sampled from glasshouse grown plants and quickly frozen in liquid nitrogen) using the NucleoSpin® RNA Plant Kit (Macherey-Nagel, Fisher Scientific, UK). cDNA was synthesized using 1 µg total RNA in 20 µl using the oligo-dT primer according to the protocol in the RevertAid Reverse Transcriptase kit (Fermentas, Life Sciences, UK). cDNA was diluted 1 in 4 to a final concentration of 12.5 ng µL⁻¹. For semi quantitative RT-PCR, 2 µL of RT reaction mixture (100 ng of RNA) in a total volume of 25 µL was used with DreamTaq DNA Polymerase (Thermo Fisher Scientific, UK) according to manufacturer's recommendations. PCR products were fractionated on 1.0% agarose gels. For qPCR, the SensiFAST SYBR No-ROX Kit was used according to manufacturer's recommendations (Bioline Reagents Ltd., London, UK). Primers used for semi quantitative RT-PCR can be seen in **Supplementary Table 1**.

Protein Extraction and immunoblot analysis

Leaf discs sampled as described above, or fresh *Porphyra umbilicalis* samples, were ground in dry ice and protein extractions performed as described in Lopez-Calcano *et al.*⁴², or using the nucleospin RNA/Protein kit (Macherey-Nagel (<http://www.mn-net.com/>) during RNA preparations. Protein quantification was performed using the protein quantification Kit from Macherey-Nagel. Samples were loaded on an equal protein basis, separated using 12% (w/v) SDS-PAGE, transferred to a nitrocellulose membrane (GE Healthcare Life science, Germany), and probed using antibodies raised against SBPase and FBP/SBPase. Proteins were detected using horseradish peroxidase conjugated to the secondary antibody and ECL chemiluminescence detection reagent (Amersham, Buckinghamshire, UK). SBPase antibodies are previously characterised^{5,43}. FBP/SBPase antibodies were raised against a peptide from a conserved region of the protein [C]-DRPRHKELIQEIRNAG-amide, and cytochrome *c*₆ antibodies were raised against peptide [C]-[Nle]-PDKTLKKDVLEANS-amide (Cambridge Research Biochemicals, Cleveland, UK). In addition to the aforementioned antibodies, samples were probed using antibodies raised against transketolase^{44,45} as loading controls.

Protein Extraction from plants for cytochrome *c*₆ analysis.

Whole leaves were harvested from 8 week old plants, washed in cold water and then wiped with a cloth soaked in 80 % ethanol to remove the majority of leaf residue. The leaves were then washed twice more in cold water, the mid rib was removed and 50 g of the remaining tissue was placed in a sealed plastic bag and stored overnight in the dark at 4°C. Proteins were extracted as in Hiyama⁴⁷, with a few modifications. Leaf tissue was homogenised in 250 ml of chilled chloroplast preparation buffer (50 mM sodium phosphate buffer, pH 7, 10 mM NaCl) for 30 seconds. The solution was then filtered through 4 layers of muslin cloth and centrifuged at 10,000 g for 5 minutes. The resulting pellet was then gently

resuspended in 50 ml of chilled chloroplast preparation buffer and the chlorophyll concentration was measured and adjusted to approximately 2 mg ml⁻¹. The resultant mixture was then added to two volumes of preheated (45°C) solubilisation medium (50 mM Tris-HCl pH 8.8 and 3% triton X) and incubated at 45°C for 30 minutes and then chilled in an ice bath for a further 30 minutes before centrifugation at 12000 g for 30 minutes. The supernatant was stored at -80°C for use in the next stage. To purify cytochrome *c*₆ protein a Biorad Econo-Pac High-Q, 5 ml type wash column was used at a flow rate of 1 ml min⁻¹. First the column was prepared by washing it with 100 ml of starting buffer (Starting buffer: 10 mM Tris-HCl pH 8.8, 0.2% triton X 100 and 20% sucrose). Then the protein mixture from the previous step was diluted with an equal volume of chilled starting buffer and passed through the column at a flow rate of 1 ml min⁻¹. Once all the protein was loaded onto the column it was then washed with 1000 ml of starting buffer supplemented with 10 mM NaCl. Then 300 ml of starting buffer supplemented with 50 mM NaCl and finally a linear gradient of starting buffer from 50 to 200 mM NaCl over a period of 4 hours at 1 ml min⁻¹ was performed and aliquots were collected. For immunoblotting, samples were acetone precipitated and the dried protein pellet then resuspended in 400 µl of solubilisation buffer (7 M urea, 2 M thiourea, 50 mM DTT, 4 % CHAPS, 0.4 % SDS, 5 mM K₂CO₃), finally 300 µl loading buffer was added (50% glycerol, 25% β-mecaptoethanol, 25% EDTA) and the samples heated at 90°C for 10 minutes before being loaded on an equal protein basis. Proteins were separated using 18% (w/v) SDS-PAGE, transferred to nitrocellulose membrane, and probed using antibodies raised against a cytochrome *c*₆ peptide. For identification of solet peak, instead of acetone precipitation, extracts were concentrated by spinning at 8,000 g and 4°C over night, using a Vivaspin 20 column (GE 28-9323-59), and a spectral scan was done in a SPECTROstar Omega plate reader from BMG Labtech.

Recombinant cytochrome c_6 protein production in *E. coli* and purification

pEC86 (CCOS Accession: CCOS891) containing *E. coli* cells were transformed with a pET28b plasmid containing the sequence for the mature cytochrome c_6 and grown in kanamycin (50 ug/ml) and chloramphenicol (35ug/ml) containing LB media. IPTG (119 $\mu\text{g ml}^{-1}$) was added to the culture when OD_{600} reached 0.5-0.6. Five hours later 330 $\mu\text{l L}^{-1}$ of 1 M ferriprotoporphyrin IX chloride was added to the media and 24 hours post IPTG, an metal ion master mix (2 mM Ni^{2+} , 2 mM Co^{2+} , 10mM Zn^{2+} , 10 mM Mn^{2+} and 50 mM Fe^{3+}) was added (1.5 ml L^{-1}). Cells were harvested after 5 days of growth and stored at -20 °C. Pellet from 500 ml was resuspended in 3 ml of lysis buffer (50mM Tris HCl pH 7.5, 1mM DTT, 1mM PMSF), sonicated (11 cycles of 30 sec sonication 30 sec rest, at 4°C) and then spun twice at 10000 g for 20 min at 4 °C. The supernatant was collected and 2 ml loaded in a 124 ml GE Hi Load 16/400 Superdex 75 pg (size exclusion) column. Protein was eluted with 0.05 M Na_2PO_4 pH 7.2, 0.5 M NaCl buffer, at a 1 ml min^{-1} speed and samples were collected every 5 ml. Fractions collected between 80-100 min were concentrated by spinning them at 8000 g over night at 4 °C using a Vivaspinn 20, (GE 28-9323-59) column. Protein concentration was determined using Bradford quantification, serial dilutions done with 50 mM Tris HCl pH 7.5 buffer and spectral scans done in a SPECTROstar Omega plate reader from BMG Labtech as with the semi-purified plant cytochrome c_6 samples.

Determination of FBPase and Transketolase Activities

FBPase activity was determined by phosphate release as described previously for SBPase with minor modifications⁸. Leaf discs were isolated from the same leaves and frozen in liquid nitrogen after photosynthesis measurements were completed. Leaf discs were ground to a fine powder in liquid nitrogen and immersed in extraction buffer (50 mM HEPES, pH8.2; 5 mM MgCl_2 ; 1 mM EDTA; 1 mM EGTA; 10% glycerol; 0.1% Triton X-

100; 2 mM benzamidine; 2 mM aminocaproic acid; 0.5 mM phenylmethylsulfonylfluoride; 10 mM dithiothreitol), centrifuged 1 min at 14,000 g, 4°C. The resulting supernatant (1 ml) was desalted through an NAP-10 column (Amersham) and stored in liquid nitrogen. The assay was carried out as described in Simkin *et al.*⁸. In brief, 20 µl of extract was added to 80 µl of assay buffer (50 mM Tris, pH 8.2; 15 mM MgCl₂; 1.5 mM EDTA; 10 mM DTT; 7.5 mM fructose-1,6-bisphosphate) and incubated at 25 °C for 30 min. The reaction was stopped by the addition of 50 µl of 1 M perchloric acid. 30 µl of samples or standards (PO₄³⁻ 0.125 to 4 nmol) were incubated 30 min at room temperature following the addition of 300 µl of Biomol Green (Affiniti Research Products, Exeter, UK) and the A620 was measured using a microplate reader (VERSAmax, Molecular Devices, Sunnyvale, CA). Activities were normalized to transketolase activity⁴⁸. For transketolase activity assays 230 µl of pre-prepared assay mix comprising of: 14.4 mM ribose-5-phosphate, 190 µM NADH, 380 µM TPP, 250 U L⁻¹ glycerol-3 phosphate dehydrogenase (G3PDH) and 6500 U L⁻¹ triose phosphate isomerase was transferred to a 96 well plate (Greiner Bio-One) and placed in a plate reader which was set at 23 °C for 5 minutes to stabilise. The plate was then ejected and 20 µl of each protein sample used for FBPase activity was injected into the wells containing the assay mix. The plate was then read for absorbance at 340 nm every 5 min for 1 hr. Activity levels were estimated by subtracting the absorbance value when the reaction becomes linear from the absorbance value 20 to 30 minutes after the first absorbance reading depending on the rate of the reaction.

Chlorophyll fluorescence imaging screening in seedlings

Chlorophyll fluorescence imaging was performed on 2-3 week-old tobacco seedlings grown in a controlled environment chamber at 130 µmol mol⁻² s⁻¹ and ambient (400 µmol mol⁻¹) CO₂. Chlorophyll fluorescence parameters were obtained using a chlorophyll

fluorescence (CF) imaging system (Technologica, Colchester, UK^{49,50}). The operating efficiency of photosystem two (PSII) photochemistry, F_q'/F_m' , was calculated from measurements of steady state fluorescence in the light (F') and maximum fluorescence (F_m') following a saturating 800 ms pulse of $6300 \mu\text{mol m}^{-2} \text{s}^{-1}$ PPFD and using the following equation $F_q'/F_m' = (F_m' - F')/F_m'$. Images of F_q'/F_m' were taken under stable PPFD of $600 \mu\text{mol m}^{-2} \text{s}^{-1}$ for Petite Havana and $650 \mu\text{mol m}^{-2} \text{s}^{-1}$ for Samsun⁵¹⁻⁵³.

Leaf Gas Exchange

Photosynthetic gas-exchange and chlorophyll fluorescence parameters were recorded using a portable infrared gas analyser (LI-COR 6400; LI-COR, Lincoln, NE, USA) with a 6400-40 fluorometer head unit. Unless stated otherwise, all measurements were taken with LI-COR 6400 cuvette. For plants grown in the glasshouse conditions were maintained at a CO_2 concentration, leaf temperature and vapour pressure deficit (VPD) of $400 \mu\text{mol mol}^{-1}$, 25°C and $1 \pm 0.2 \text{ kPa}$ respectively. The chamber conditions for plants grown under field conditions had a CO_2 concentration of $400 \mu\text{mol mol}^{-1}$, block temperature was set to 2°C above ambient temperature (ambient air temperature was measure before each curve) and VPD was maintained as close to 1 kPa as feasible possible.

A/C_i response curves (Photosynthetic capacity)

The response of net photosynthesis (A) to intracellular CO_2 concentration (C_i) was measured at a saturating light intensity of $2000 \mu\text{mol mol}^{-2} \text{s}^{-1}$. Illumination was provided by a red-blue light source attached to the leaf cuvette. Measurements of A were started at ambient CO_2 concentration (C_a) of $400 \mu\text{mol mol}^{-1}$, before C_a was decreased step-wise to a lowest concentration of $50 \mu\text{mol mol}^{-1}$ and then increased step-wise to an upper concentration of $2000 \mu\text{mol mol}^{-1}$. To calculate the maximum saturated CO_2 assimilation rate (A_{max}),

maximum carboxylation rate ($V_{c_{\max}}$) and maximum electron transport flow (J_{\max}), the C3 photosynthesis model⁵⁴ was fitted to the A/C_i data using a spreadsheet provided by Sharkey *et al.*⁵⁵. Additionally, chlorophyll fluorescence parameters including PSII operating efficiency (F_q'/F_m') and the coefficient of photochemical quenching (q_P), mathematically identical to the PSII efficiency factor (F_q'/F_v') were recorded at each point.

***A/Q* response curves**

Photosynthesis as a function of light (*A/Q* response curves) was measured under the same cuvette conditions as the A/C_i curves mentioned above. Leaves were initially stabilized at saturating irradiance of 2200 to $\mu\text{mol m}^{-2} \text{s}^{-1}$, after which A and g_s were measured at the following light levels: 2000, 1650, 1300, 1000, 750, 500, 400, 300, 200, 150, 100, 50 and 0 $\mu\text{mol m}^{-2} \text{s}^{-1}$). Measurements were recorded after A reached a new steady state (1-3 min) and before g_s changed to the new light levels. Values of A and g_s were used to estimate intrinsic water-use efficiency ($iWUE = A/g_s$)

Monitoring electron transport and assimilation during light changes.

A DUAL-PAM attached to a GFS-3000 (Walz, Effeltrich, Germany) was used to monitor the response of the effective photochemical quantum yield of PSII (F_q'/F_m') and PSI ($Y(I)$), and the net CO_2 Assimilation (A) to changes in light intensity. To remove stomatal limitation of A , plants were maintained at constant temperature (24°C), relative humidity (60%) and high $[\text{CO}_2]$ (1500 $\mu\text{mol mol}^{-1}$). Plants were dark adapted and the induction/relaxation of the photosystems was tested by subjecting plants to a step change in light intensity from 0 to 1000 $\mu\text{mol m}^{-2} \text{s}^{-1}$, this intensity was maintained for 5 min before returning to dark.

Statistical Analysis

All statistical analyses were done using Sys-stat, University of Essex, UK, and R (<https://www.r-project.org/>). For greenhouse and the 2016 field experiment biomass data, seedling chlorophyll imaging and enzyme activities, analysis of variance and Post hoc Tukey tests were done. For gas exchange curves, data were compared by linear mixed model analysis using lmer function and type III anova⁵⁶. Significant differences between manipulations were identified using contrasts analysis (lsmeans package). For the 2017 field experiments, biomass data were compared by linear mixed model analysis using lmer function and type III anova to account for block effect using four plants/genotype for n=6 blocks. For the analysis of electron transport and assimilation during light changes, the slope of the activation curves was calculated for each parameter and analysis of variance and post-hoc Tukey test was done.

Data availability

The data that support the findings of this study, plant transformation constructs and seed are available from the corresponding authors on reasonable request.

Figure Legends**Fig. 1. Screening of transgenic plants overexpressing FBP/SBPase, SBPase, and cytochrome c_6 .**

(a) Immunoblot analysis of protein extracts from mature leaves of evaluated S_B , $S_B C_6$, S and SC_6 lines compared to wild type and azygous (control, CN) plants, using FBP/SBPase and SBPase antibodies. Equal amounts of protein were loaded, Transketolase (TK) is the loading control. Repeated 3 times with similar results. (b) Immunoblot analysis of Cytochrome c_6 protein extract from mature leaves of C_6 compared to CN plants, ponceau staining was used as loading control for plant samples only. Additionally, a crude *Porphyra sp.* protein extract is presented as confirmation of correct band size for the introduced Cytochrome c_6 . Repeated 3 times with similar results (c) FBPase activity in S_B (n=16) and $S_B C_6$ (n=14) relative to CN (n=6) plants. Chlorophyll fluorescence imaging of plants grown in controlled environmental conditions was used to determine F_q'/F_m' (maximum PSII operating efficiency) at 600-650 $\mu\text{mol m}^{-2} \text{s}^{-1}$, 14 to 21 days after sowing (d) CN (n=20), S_B (n= 28), C_6 (n=29), $S_B C_6$ (n=30), (e) CN (n=11), S (n=7) and SC_6 (n=6). Mean and SE is presented. Statistical tests used analysis of variance and post-hoc Tukey test.

Fig 2. Photosynthetic responses of transgenic plants grown in the glasshouse.

Photosynthetic carbon fixation rates, operating efficiency of PSII in the light (F_q'/F_m'), PSII efficiency factor (F_q'/F_v') and PSII maximum efficiency (F_v'/F_m') are presented in (a) mature leaves CN (n=10), S_B (n=7), C_6 (n=11), $S_B C_6$ (n=9) cv. Petit Havana (b) mature leaves of CN (n=10), S (n=8), SC_6 (n=10) and (c) developing leaves CN (n=6), S (n=6), SC_6 (n=9) cv.

Samsun. Parameters were determined as a function of increasing CO₂ concentrations at saturating-light levels in developing (11-13cm in length) and mature leaves. Plants were grown in the glasshouse where light levels oscillated between 400 and 1000 $\mu\text{mol m}^{-2} \text{s}^{-1}$ (supplemental light ensured a minimum of 400 $\mu\text{mol m}^{-2} \text{s}^{-1}$). Control group (CN) represent both WT and azygous plants. Asterisks indicate significance between the transgenics and CN plants, using a linear mixed-effects model and type III ANOVA and contrast analysis, *p < 0.05, exact p value indicated in each plot.

Figure 3. Increased SBPase or expression of FBP/SBPase and cytochrome *c₆* increases biomass in glasshouse grown plants.

Tobacco plants were germinated in growth cabinets and moved to the glasshouse at 10-14 d post-germination. Forty-day-old (cv. Petit Havana) or fifty-six-day-old (cv. Samsun) plants were harvested and plant height, leaf area and above-ground biomass (dry weight) determined. Control group represent both WT and azygous plants (CN). cv. Petite Havana CN (n=17), S_B (n=21), C₆ (n=18), (S_BC₆ n=18); cv. Samsun CN (n= 16), S (n=7, SC₆ (n= 13). Mean and SE is presented. Statistical analysis was ANOVA with post-hoc Tukey test.

Figure 4. Simultaneous expression of FBP/SBPase and cytochrome *c₆* increases biomass in field grown plants.

(a-c) Forty-day-old (young) 2016 field-grown plants (plants were germinated and grown in glasshouse conditions for 26 d and then allowed to grow in the field in summer 2016 for 14 d); (d-i) Fifty-seven-day-old or sixty-one-day-old (flowering) 2017 field-grown plants (plants were germinated and grown in glasshouse conditions for 26 d and grown in the field in summer 2017 until flowering established, circa 30 d). Plant height, leaf area and total above-ground biomass (dry weight) are shown. 2016 Experiment CN (n=72), S_B (n=33), C₆ (n=33);

2017 Experiment 1: CN (n=93), S_B (n=71), C₆ (n=70); 2017 Experiment 2: (n=97), C₆ (n=72), S_BC₆ (n=47) Mean ± SE presented. Statistical analysis was ANOVA with post-hoc Tukey test.

Fig 5. Photosynthetic capacity of field-grown transgenic plants.

Photosynthetic carbon fixation rates and operating efficiency of PSII as a function of increasing CO₂ concentrations at saturating-light levels in mature leaves from CN and transgenic plants. (a) 2017 experiment 1: CN (n= 21), S_B (n=16) and C₆ (n=16). (b) 2017 experiment 2: Lines expressing cytochrome CN (n=22) C₆ (n=16), S_BC₆ (n=14). Control group (CN) represent both WT and azygous plants. Mean ± SE presented. A linear mixed-effects model and type III ANOVA was applied, exact p value indicated in each plot.

Fig 6. Simultaneous expression of FBP/SBPase and cytochrome *c₆* can increase water use efficiency under field conditions.

(a) Net CO₂ assimilation rate (*A*), (b) Stomatal conductance (*g_s*), (c) Intercellular CO₂ concentration (*C_i*), and (d) Intrinsic water-use efficiency (*iWUE*) as a function of light (PPFD) in field-grown plants, CN n= 22, C₆ n=16, S_BC₆ n=14. A linear mixed-effects model and type III ANOVA was applied, exact p value indicated in each plot.

Table 1. Maximum electron transport and RuBP regeneration rate (J_{\max}), maximum carboxylation rate of Rubisco ($V_{c\max}$) and maximum assimilation (A_{\max}) of WT and transgenic lines. Results were determined from the A/C_i curves in Figure 2 using the equations published by von Caemmerer and Farquhar⁵⁷. Significant differences are shown in boldface (* $p < 0.05$). cv. Samsun Mature leaves CN (n=10), S (n=8), SC₆ (n=10); developing leaves CN (n=6), S (n=6), SC₆ (n=9); cv. Petit Havana Mature leaves: CN (n=10), S_B (n=7), C₆ (n=11), S_BC₆ (n=9) Mean and SE are shown.

A/C_i				
Leaf Stage	Line	$V_{c\max}$ ($\mu\text{mol m}^{-2} \text{s}^{-1}$)	J_{\max} ($\mu\text{mol m}^{-2} \text{s}^{-1}$)	A_{\max} ($\mu\text{mol m}^{-2} \text{s}^{-1}$)
Developing	CN	72.32 \pm 5.5	157.51 \pm 6.0	29.6 \pm 1.1
	S	87.7 \pm 4.3	179.8 \pm 4.9*	34.1 \pm 0.7*
	SC ₆	86.5 \pm 3.5	181.2 \pm 3.6*	33.7 \pm 1.1*
Samsun				
Mature	CN	77.2 \pm 3.3	171.0 \pm 6.0	31.6 \pm 1.0
	S	81.3 \pm 6.1	183.5 \pm 9.0	32.2 \pm 0.7
	SC ₆	90.3 \pm 3.3	193.1 \pm 5.4	34.9 \pm 1.1*
Petit Havana	CN	69.6 \pm 2.0	121.5 \pm 1.3	24.6 \pm 0.5
	S _B	69.0 \pm 5.1	128.7 \pm 3.8	27.0 \pm 0.8
	C ₆	79.3 \pm 7.0	129.9 \pm 5.1	25.6 \pm 0.5
	S _B C ₆	76.5 \pm 4.2	132.0 \pm 3.8	27.4 \pm 0.8*

675 **References**

676

- 677 1 Zhu, X. G., Long, S. P. & Ort, D. R. Improving photosynthetic efficiency for greater
678 yield. *Annu Rev Plant Biol* **61**, 235-261, doi:10.1146/annurev-arplant-042809-112206
679 (2010).
- 680 2 Simkin, A. J., Lopez-Calcagno, P. E. & Raines, C. A. Feeding the world: Improving
681 photosynthetic efficiency for sustainable crop production. *Journal of Experimental*
682 *Botany*, doi:doi.org/10.1093/jxb/ery445 (2019).
- 683 3 Simkin, A. J. Genetic Engineering for Global Food Security: Photosynthesis and
684 Biofortification. *Plants* **8**, 586 (2019).
- 685 4 Miyagawa, Y., Tamoi, M. & Shigeoka, S. Overexpression of a cyanobacterial
686 fructose-1,6-/sedoheptulose-1,7-bisphosphatase in tobacco enhances photosynthesis
687 and growth. *Nat Biotechnol* **19**, 965-969, doi:10.1038/nbt1001-965 (2001).
- 688 5 Lefebvre, S. *et al.* Increased sedoheptulose-1,7-bisphosphatase activity in transgenic
689 tobacco plants stimulates photosynthesis and growth from an early stage in
690 development. *Plant physiology* **138**, 451-460, doi:10.1104/pp.104.055046 (2005).
- 691 6 Raines, C. A. Transgenic approaches to manipulate the environmental responses of
692 the C(3) carbon fixation cycle. *Plant Cell Environ* **29**, 331-339, doi:10.1111/j.1365-
693 3040.2005.01488.x (2006).
- 694 7 Rosenthal, D. M. *et al.* Over-expressing the C(3) photosynthesis cycle enzyme
695 Sedoheptulose-1-7 Bisphosphatase improves photosynthetic carbon gain and yield
696 under fully open air CO(2) fumigation (FACE). *BMC Plant Biol* **11**, 123,
697 doi:10.1186/1471-2229-11-123 (2011).
- 698 8 Simkin, A. J., McAusland, L., Headland, L. R., Lawson, T. & Raines, C. A.
699 Multigene manipulation of photosynthetic carbon assimilation increases CO₂ fixation
700 and biomass yield in tobacco. *J Exp Bot* **66**, 4075-4090, doi:10.1093/jxb/erv204
701 (2015).
- 702 9 Simkin, A. J. *et al.* Simultaneous stimulation of sedoheptulose 1,7-bisphosphatase,
703 fructose 1,6-bisphosphate aldolase and the photorespiratory glycine decarboxylase-H
704 protein increases CO₂ assimilation, vegetative biomass and seed yield in Arabidopsis.
705 *Plant Biotechnol J* **15**, 805-816, doi:10.1111/pbi.12676 (2017).
- 706 10 Zhu, X. G., de Sturler, E. & Long, S. P. Optimizing the distribution of resources
707 between enzymes of carbon metabolism can dramatically increase photosynthetic
708 rate: A numerical simulation using an evolutionary algorithm. *Plant physiology* **145**,
709 513-526, doi:DOI 10.1104/pp.107.103713 (2007).
- 710 11 Long, S. P., Zhu, X. G., Naidu, S. L. & Ort, D. R. Can improvement in photosynthesis
711 increase crop yields? *Plant Cell Environ* **29**, 315-330 (2006).
- 712 12 Poolman, M. G., Fell, D. A. & Thomas, S. Modelling photosynthesis and its control. *J*
713 *Exp Bot* **51**, 319-328, doi:DOI 10.1093/jexbot/51.suppl_1.319 (2000).
- 714 13 Raines, C. A. The Calvin cycle revisited. *Photosynth Res* **75**, 1-10, doi:Doi
715 10.1023/A:1022421515027 (2003).
- 716 14 Uematsu, K., Suzuki, N., Iwamae, T., Inui, M. & Yukawa, H. Increased fructose 1,6-
717 bisphosphate aldolase in plastids enhances growth and photosynthesis of tobacco
718 plants. *J Exp Bot* **63**, 3001-3009, doi:10.1093/jxb/ers004 (2012).
- 719 15 Ding, F., Wang, M. L., Zhang, S. X. & Ai, X. Z. Changes in SBPase activity
720 influence photosynthetic capacity, growth, and tolerance to chilling stress in
721 transgenic tomato plants. *Sci Rep-Uk* **6**, doi:ARTN 32741
722 10.1038/srep32741 (2016).

- 723 16 Driever, S. M. *et al.* Increased SBPase activity improves photosynthesis and grain
724 yield in wheat grown in greenhouse conditions. *Philosophical Transactions of the*
725 *Royal Society B* **372**, 1730 (2017).
- 726 17 Tamoi, M., Nagaoka, M., Miyagawa, Y. & Shigeoka, S. Contribution of fructose-1,6-
727 bisphosphatase and sedoheptulose-1,7-bisphosphatase to the photosynthetic rate and
728 carbon flow in the Calvin cycle in transgenic plants. *Plant Cell Physiology* **47**, 380-
729 390, doi:10.1093/pcp/pcj004 (2006).
- 730 18 Ichikawa, Y. *et al.* Generation of transplastomic lettuce with enhanced growth and
731 high yield. *GM Crops* **1**, 322-326, doi:10.4161/gmcr.1.5.14706 (2010).
- 732 19 Kohler, I. H. *et al.* Expression of cyanobacterial FBP/SBPase in soybean prevents
733 yield depression under future climate conditions. *J Exp Bot* **68**, 715-726,
734 doi:10.1093/jxb/erw435 (2017).
- 735 20 Simkin, A. J., McAusland, L., Lawson, T. & Raines, C. A. Overexpression of the
736 RieskeFeS Protein Increases Electron Transport Rates and Biomass Yield. *Plant*
737 *Physiol* **175**, 134-145, doi:10.1104/pp.17.00622 (2017).
- 738 21 Ermakova, M., Lopez-Calcano, P. E., Raines, C. A., Furbank, R. T. & von
739 Caemmerer, S. Overexpression of the Rieske FeS protein of the Cytochrome *b₆*
740 complex increases C4 photosynthesis in *Setaria viridis*. *Communications Biology* **2**,
741 314, doi:10.1038/s42003-019-0561-9 (2019).
- 742 22 Chida, H. *et al.* Expression of the algal cytochrome *c₆* gene in Arabidopsis enhances
743 photosynthesis and growth. *Plant & cell physiology* **48**, 948-957,
744 doi:10.1093/pcp/pcm064 (2007).
- 745 23 Yadav, S. K., Khatri, K., Rathore, M. S. & Jha, B. Introgression of UfCyt *c₆*, a
746 thylakoid lumen protein from a green seaweed *Ulva fasciata* Delile enhanced
747 photosynthesis and growth in tobacco. *Molecular biology reports* **45(6)**, 1745-1758,
748 doi:10.1007/s11033-018-4318-1 (2018).
- 749 24 Merchant, S. & Bogorad, L. The Cu(II)-repressible plastidic cytochrome *c*. Cloning
750 and sequence of a complementary DNA for the pre-apoprotein. *Journal of Biological*
751 *Chemistry* **262**, 9062-9067 (1987).
- 752 25 De la Rosa M.A., M.-H. F. P., Hervás M., Navarro J.A. Convergent Evolution of
753 Cytochrome *c₆* and Plastocyanin. In: *Golbeck J.H. (eds) Photosystem I. Advances in*
754 *Photosynthesis and Respiration*, vol 24. Springer, Dordrecht (2006).
- 755 26 Finazzi, G., Sommer, F. & Hippler, M. Release of oxidized plastocyanin from
756 photosystem I limits electron transfer between photosystem I and cytochrome *b₆*
757 complex in vivo. *Proc Natl Acad Sci U S A* **102**, 7031-7036,
758 doi:10.1073/pnas.0406288102 (2005).
- 759 27 Gong, H. Y. *et al.* Transgenic Rice Expressing Ictb and FBP/Sbpase Derived from
760 Cyanobacteria Exhibits Enhanced Photosynthesis and Mesophyll Conductance to
761 CO₂. *Plos One* **10**, doi:ARTN e0140928
762 10.1371/journal.pone.0140928 (2015).
- 763 28 Yadav, S. K., Khatri, K., Rathore, M. S. & Jha, B. Introgression of UfCyt *c₆*, a
764 thylakoid lumen protein from a green seaweed *Ulva fasciata* Delile enhanced
765 photosynthesis and growth in tobacco. *Mol Biol Rep*, doi:10.1007/s11033-018-4318-1
766 (2018).
- 767 29 Wullschleger, S. D. Biochemical Limitations to Carbon Assimilation in C(3) Plants -
768 a Retrospective Analysis of the A/Ci Curves from 109 Species. *J Exp Bot* **44**, 907-
769 920, doi:DOI 10.1093/jxb/44.5.907 (1993).
- 770 30 Pesaresi, P. *et al.* Mutants, Overexpressors, and Interactors of Arabidopsis
771 Plastocyanin Isoforms: Revised Roles of Plastocyanin in Photosynthetic Electron

- Flow and Thylakoid Redox State. *Mol Plant* **2**, 236-248, doi:10.1093/mp/ssn041 (2009).
- 31 López-Calcano, P. E. *et al.* Overexpressing the H⁺ protein of the glycine cleavage system increases biomass yield in glasshouse and field-grown transgenic tobacco plants. *Plant biotechnology journal* **17**, 141-151, doi:doi.org/10.1111/pbi.12953 (2018).
- 32 Glowacka, K. *et al.* Photosystem II Subunit S overexpression increases the efficiency of water use in a field-grown crop. *Nat Commun* **9**, doi:ARTN 868 10.1038/s41467-018-03231-x (2018).
- 33 Busch, F. A. Opinion: The red-light response of stomatal movement is sensed by the redox state of the photosynthetic electron transport chain. *Photosynth Res* **119**, 131-140, doi:10.1007/s11120-013-9805-6 (2014).
- 34 Engler, C., Gruetzner, R., Kandzia, R. & Marillonnet, S. Golden Gate Shuffling: A One-Pot DNA Shuffling Method Based on Type IIs Restriction Enzymes. *Plos One* **4**, doi:ARTN e5553 10.1371/journal.pone.0005553 (2009).
- 35 Engler, C., Kandzia, R. & Marillonnet, S. A one pot, one step, precision cloning method with high throughput capability. *Plos One* **3**, e3647, doi:10.1371/journal.pone.0003647 (2008).
- 36 Nakagawa, T. *et al.* Development of series of gateway binary vectors, pGWBs, for realizing efficient construction of fusion genes for plant transformation. *Journal of bioscience and bioengineering* **104**, 34-41, doi:10.1263/jbb.104.34 (2007).
- 37 Simkin, A. J. *et al.* Characterization of the plastidial geraniol synthase from *Madagascar periwinkle* which initiates the monoterpenoid branch of the alkaloid pathway in internal phloem associated parenchyma. *Phytochemistry* **85**, 36-43, doi:10.1016/j.phytochem.2012.09.014 (2013).
- 38 Richins, R. D., Scholthof, H. B. & Shepherd, R. J. Sequence of Figwort Mosaic-Virus DNA (Caulimovirus Group). *Nucleic acids research* **15**, 8451-8466, doi:DOI 10.1093/nar/15.20.8451 (1987).
- 39 Horsch, R. B., Rogers, S. G. & Fraley, R. T. Transgenic Plants - Technology and Applications. *Abstr Pap Am Chem S* **190**, 67 (1985).
- 40 Hoagland, D. R. & Arnon, D. I. *The water-culture method for growing plants without soil*. (The College of Agriculture, 1950).
- 41 Kromdijk, J. *et al.* Improving photosynthesis and crop productivity by accelerating recovery from photoprotection. *Science* **354**, 857-861, doi:10.1126/science.aai8878 (2016).
- 42 Lopez-Calcano, P. E., Abuzaid, A. O., Lawson, T. & Raines, C. A. Arabidopsis CP12 mutants have reduced levels of phosphoribulokinase and impaired function of the Calvin-Benson cycle. *J Exp Bot* **68**, 2285-2298, doi:10.1093/jxb/erx084 (2017).
- 43 Dunford, R. P., Catley, M. A., Raines, C. A., Lloyd, J. C. & Dyer, T. A. Purification of active chloroplast sedoheptulose-1,7-bisphosphatase expressed in *Escherichia coli*. *Protein expression and purification* **14**, 139-145, doi:10.1006/prep.1998.0939 (1998).
- 44 Henkes, S., Sonnewald, U., Badur, R., Flachmann, R. & Stitt, M. A small decrease of plastid transketolase activity in antisense tobacco transformants has dramatic effects on photosynthesis and phenylpropanoid metabolism. *The Plant cell* **13**, 535-551 (2001).
- 45 Khozaei, M. *et al.* Overexpression of plastid transketolase in tobacco results in a thiamine auxotrophic phenotype. *The Plant cell* **27**, 432-447, doi:10.1105/tpc.114.131011 (2015).

- 821 46 Timm, S. *et al.* Glycine decarboxylase controls photosynthesis and plant growth.
822 *FEBS letters* **586**, 3692-3697, doi:10.1016/j.febslet.2012.08.027 (2012).
- 823 47 Hiyama, T. Isolation of photosystem I particles from spinach. *Methods Mol Biol* **274**,
824 11-17, doi:10.1385/1-59259-799-8:011 (2004).
- 825 48 Zhao, Y. L. *et al.* Downregulation of Transketolase Activity Is Related to Inhibition
826 of Hippocampal Progenitor Cell Proliferation Induced by Thiamine Deficiency.
827 *Biomed Res Int*, doi:Artn 572915
828 10.1155/2014/572915 (2014).
- 829 49 Barbagallo, R. P., Oxborough, K., Pallett, K. E. & Baker, N. R. Rapid, noninvasive
830 screening for perturbations of metabolism and plant growth using chlorophyll
831 fluorescence imaging. *Plant physiology* **132**, 485-493, doi:10.1104/pp.102.018093
832 (2003).
- 833 50 von Caemmerer, S. *et al.* Stomatal conductance does not correlate with photosynthetic
834 capacity in transgenic tobacco with reduced amounts of Rubisco. *J Exp Bot* **55**, 1157-
835 1166, doi:10.1093/jxb/erh128 (2004).
- 836 51 Baker, N. R., Oxborough, K., Lawson, T. & Morison, J. I. L. High resolution imaging
837 of photosynthetic activities of tissues, cells and chloroplasts in leaves. *Journal of*
838 *Experimental Botany* **52**, 615-621 (2001).
- 839 52 Oxborough, K. & Baker, N. R. An evaluation of the potential triggers of
840 photoinactivation of photosystem II in the context of a Stern–Volmer model for
841 downregulation and the reversible radical pair equilibrium model. *Philosophical*
842 *Transactions of the Royal Society of London. Series B: Biological Sciences* **355**, 1489-
843 1498 (2000).
- 844 53 Lawson, T., Lefebvre, S., Baker, N. R., Morison, J. I. L. & Raines, C. A. Reductions
845 in mesophyll and guard cell photosynthesis impact on the control of stomatal
846 responses to light and CO₂. *J Exp Bot* **59**, 3609-3619, doi:10.1093/jxb/ern211
847 (2008).
- 848 54 Farquhar, G., von Caemmerer, S. v. & Berry, J. A biochemical model of
849 photosynthetic CO₂ assimilation in leaves of C₃ species. *Planta* **149**, 78-90 (1980).
- 850 55 Sharkey, T. D., Bernacchi, C. J., Farquhar, G. D. & Singsaas, E. L. Fitting
851 photosynthetic carbon dioxide response curves for C₃ leaves. *Plant Cell Environ* **30**,
852 1035-1040, doi:10.1111/j.1365-3040.2007.01710.x (2007).
- 853 56 Vialet-Chabrand, S., Matthews, J. S. A., Simkin, A. J., Raines, C. A. & Lawson, T.
854 Importance of Fluctuations in Light on Plant Photosynthetic Acclimation. *Plant*
855 *physiology* **173**, 2163-2179, doi:10.1104/pp.16.01767 (2017).
- 856 57 von Caemmerer, S. & Farquhar, G. D. Some Relationships between the Biochemistry
857 of Photosynthesis and the Gas-Exchange of Leaves. *Planta* **153**, 376-387, doi:Doi
858 10.1007/Bf00384257 (1981).
- 859

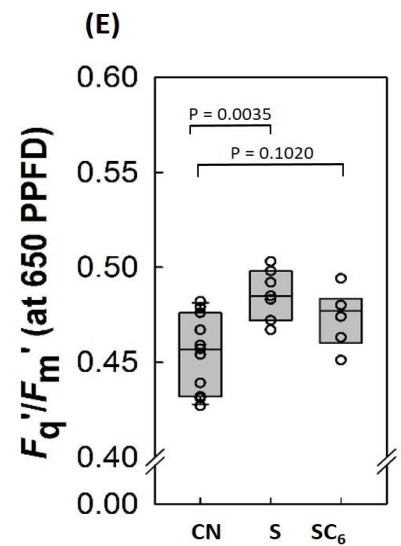
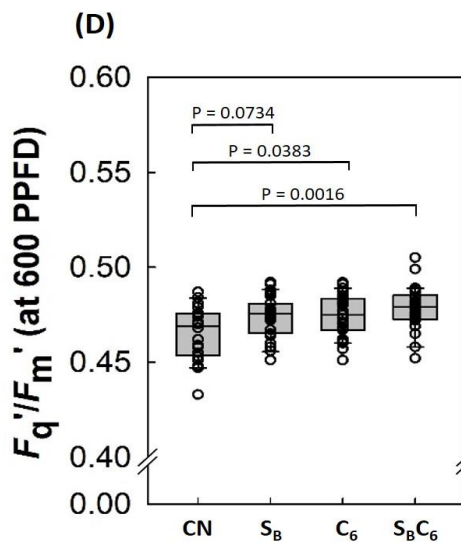
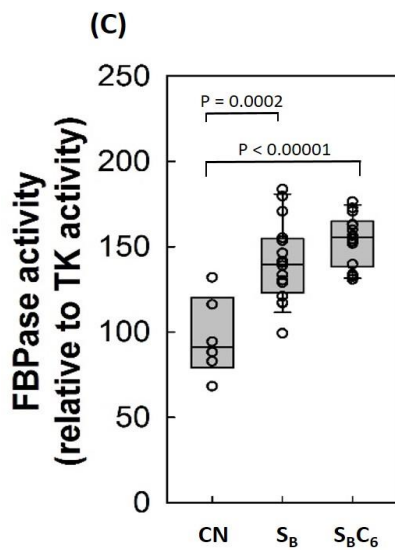
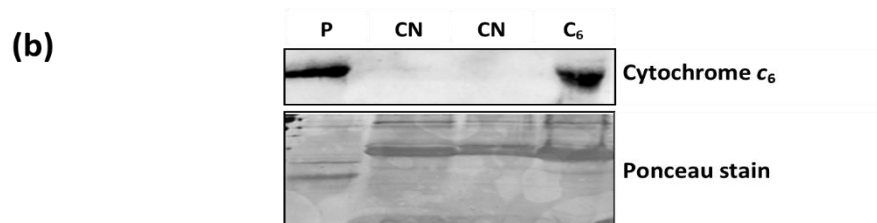
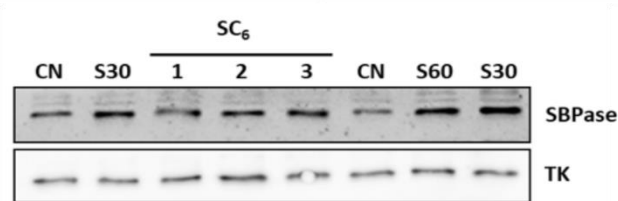
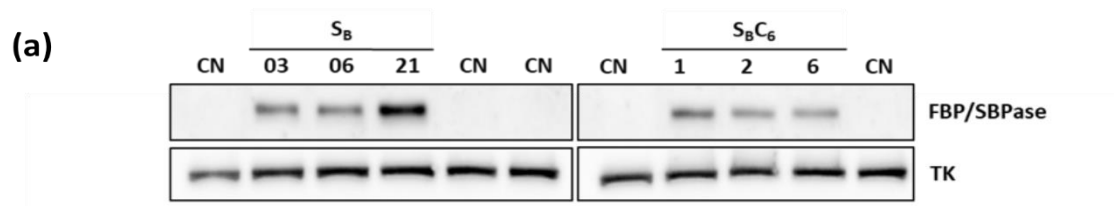
Acknowledgments

This study was supported by the Realising Improved Photosynthetic Efficiency (RIPE) initiative awarded to C.A.R by University of Illinois, USA. RIPE was possible through support from the Bill & Melinda Gates Foundation, DFID and FFAR, grant OPP1172157. This work was also supported by the Biotechnology and Biological Sciences Research Council (BBSRC) grant BB/J004138/1. We would like to thank Jack Matthews (University of Essex) for help with data analysis, Elena A. Pelech (University of Illinois) and Sunitha Subramaniam (University of Essex) for help with plant growth, Phillip A. Davey (University of Essex) and Richard Gossen (University of Helsinki) for help with gas exchange and David Drag, Ben Harbaugh and the Ort lab (University of Illinois) for support with the field trials.

Author contributions

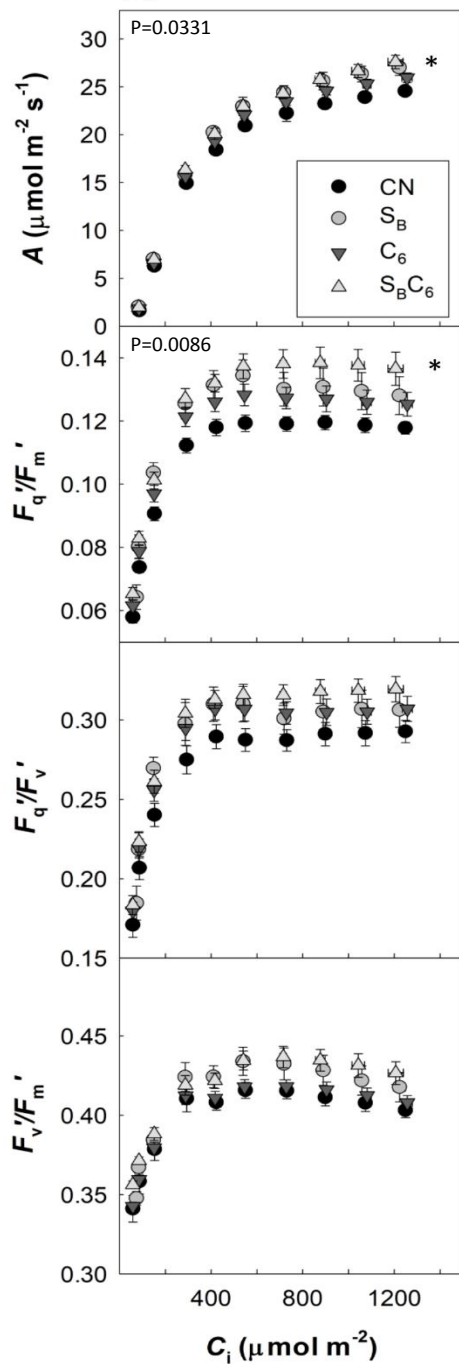
P.E.L.C and A.J.S. generated transgenic plants. P.E.L.C, A.J.S, K.L.B. and S.J.F. performed molecular and biochemical experiments. P.E.L.C, A.J.S and K.L.B carried out plant phenotypic and growth analysis and performed gas exchange measurement, S.V.C. made the measurements of photosynthesis during light induction. A.J.S and S.J.F performed enzyme assays on selected lines; all authors carried out data analysis on their respective contributions; C.A.R and T.L designed and supervised the research; P.E.L.C., A.J.S and C.A.R wrote the manuscript, TL contributed to editing of the manuscript and finalising of figures. P.E.L.C, K.L.B. and A.J.S contributed equally to the completion of this work.

Competing interests: The authors declare no competing financial interests



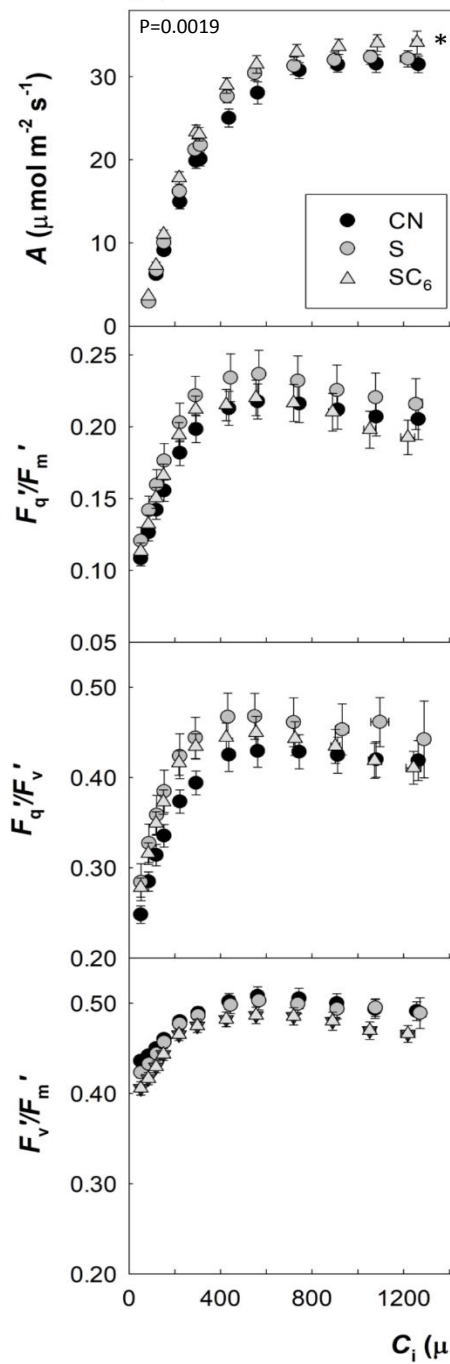
cv. Petite Havana

(a) Mature leaf

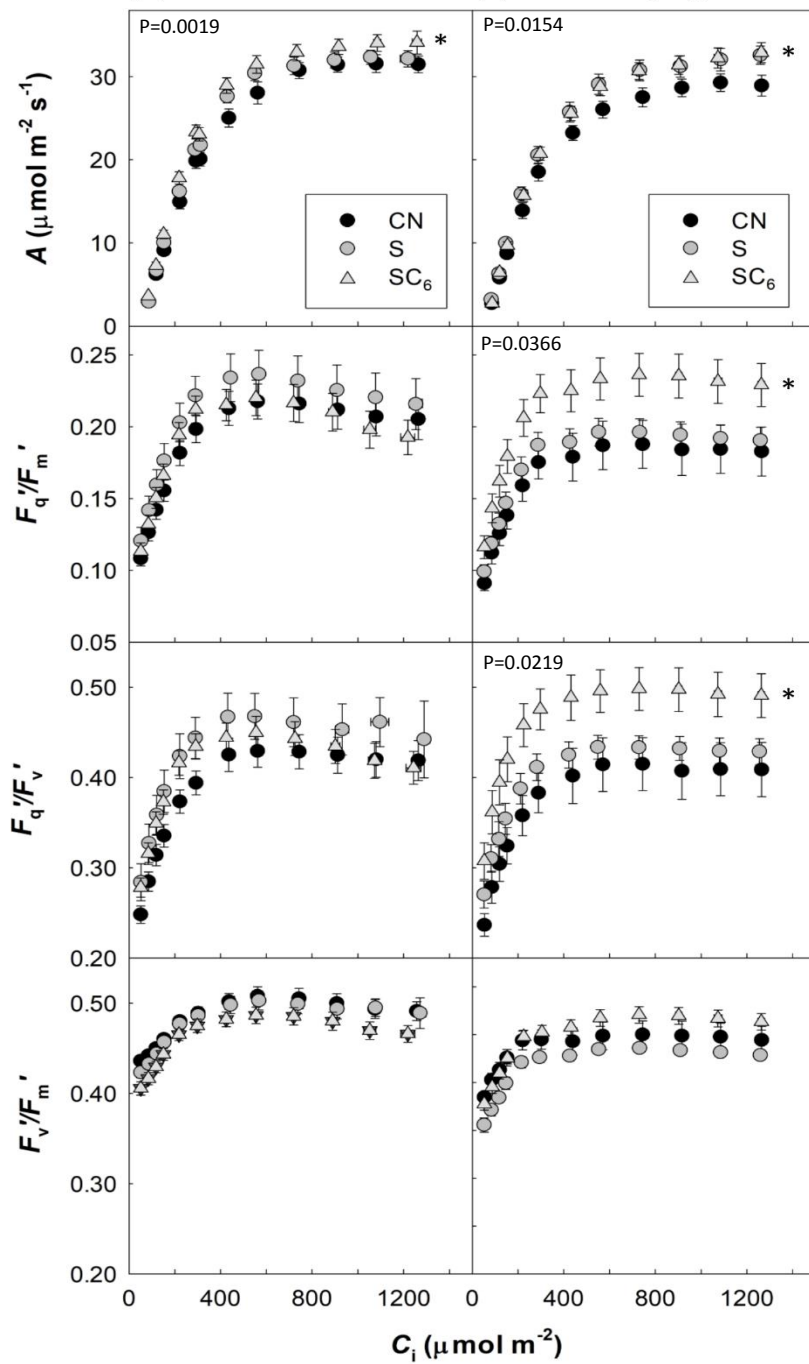


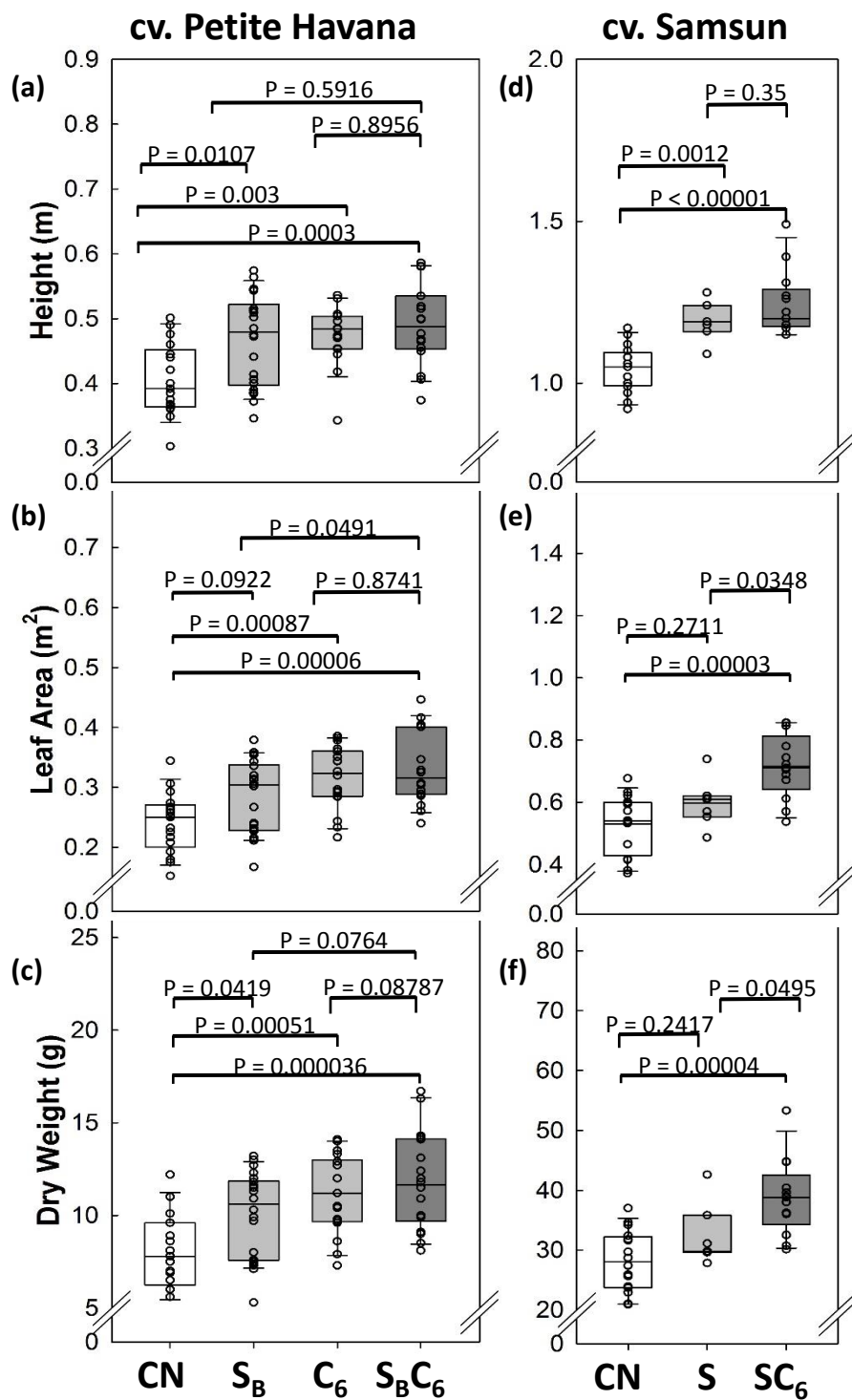
cv. Samsun

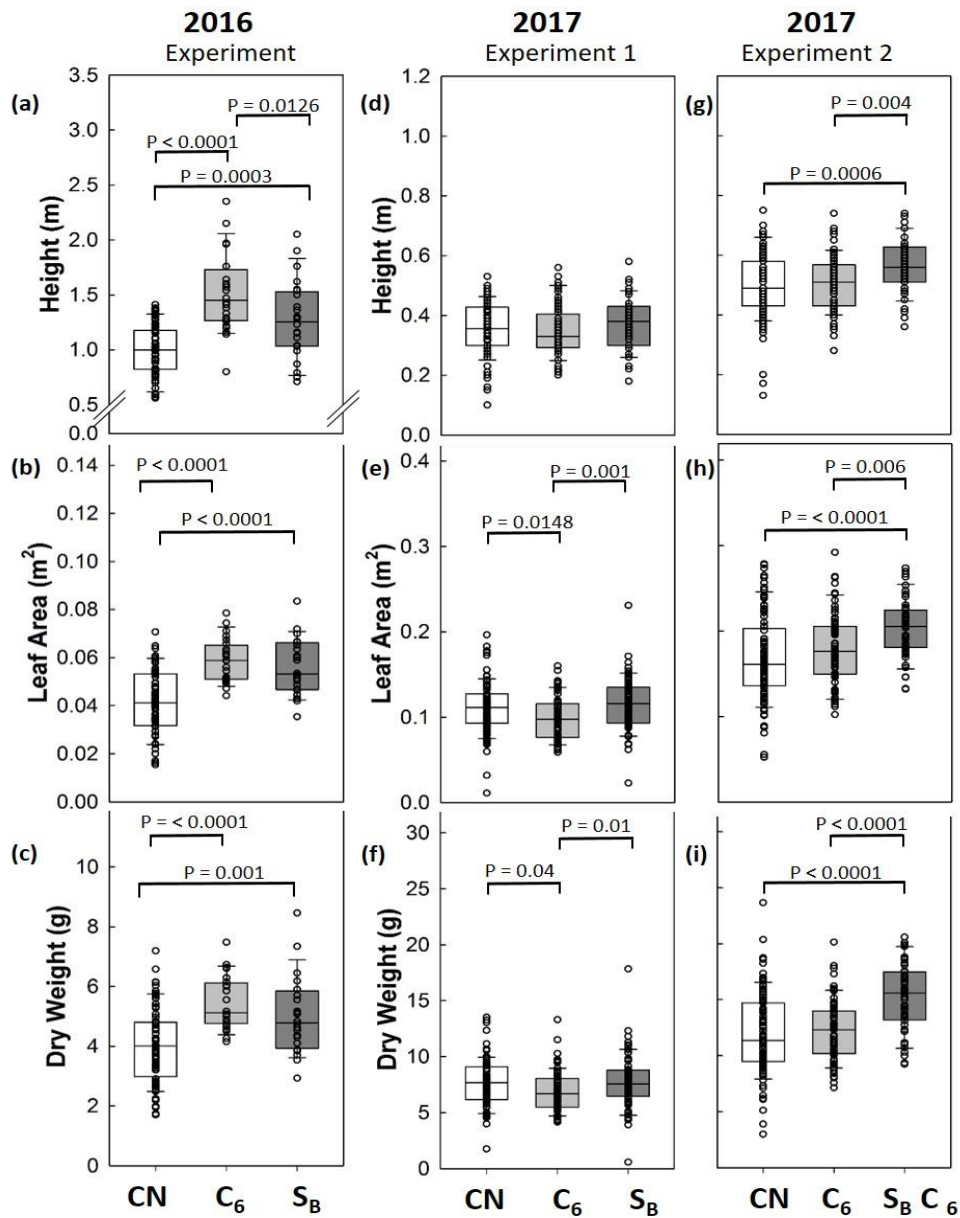
(b) Mature leaf

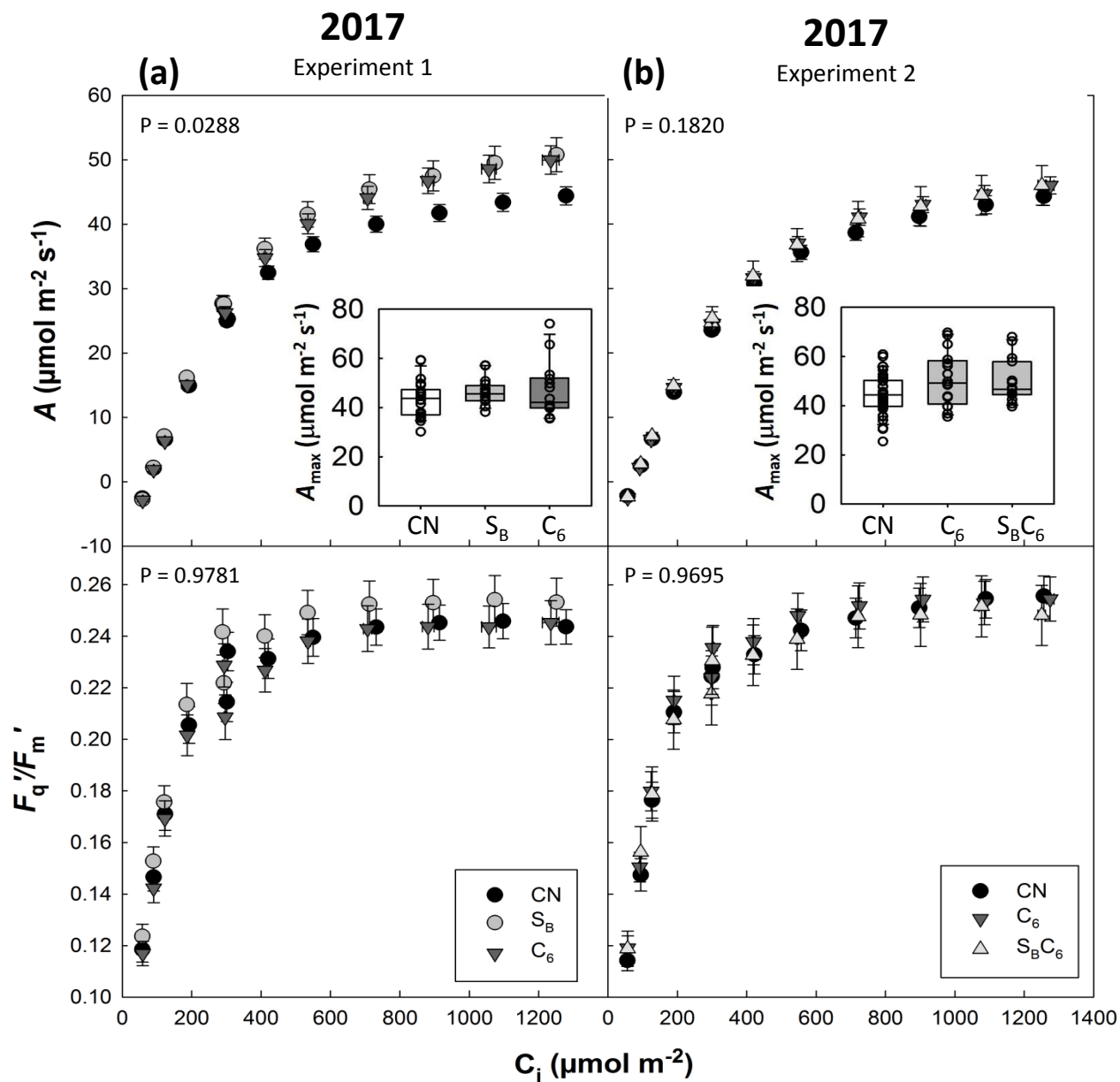


(c) Developing leaf









2017

Experiment 2

